

Spin-dependent Parton Distributions from Polarized Structure Function Data

T. Gehrmann

*Department of Physics, University of Durham
Durham DH1 3LE, England*

and

W.J. Stirling

*Departments of Physics and Mathematical Sciences, University of Durham
Durham DH1 3LE, England*

Abstract

In the past year, polarized deep inelastic scattering experiments at CERN and SLAC have obtained structure function measurements off proton, neutron and deuteron targets at a level of precision never before achieved. The measurements can be used to test the Bjorken and Ellis-Jaffe sum rules, and also to obtain information on the parton distributions in polarized nucleons. We perform a global leading-order QCD fit to the proton deep inelastic data in order to extract the spin-dependent parton distributions. By using parametric forms which are consistent with theoretical expectations at large and small x , we find that the quark distributions are now rather well constrained. We assume that there is no significant intrinsic polarization of the strange quark sea. The data are then consistent with a modest amount of the proton's spin carried by the gluon, although the shape of the gluon distribution is not well constrained, and several qualitatively different shapes are suggested. The spin-dependent distributions we obtain can be used as input to phenomenological studies for future polarized hadron-hadron and lepton-hadron colliders.

1 Introduction

In the last few years there has been a resurgence of interest in the spin structure of the nucleon. This was largely initiated by the measurements of the polarized structure function g_1^p by the SLAC-Yale [1] and EMC [2] collaborations. In the ‘naive’ parton model, g_1 can, like the unpolarized structure function F_1 , be expressed in terms of the probability distributions for finding quarks with spin parallel or antiparallel to the longitudinally polarized parent proton:

$$F_1(x, Q^2) = \frac{1}{2} \sum_q e_q^2 [q(x) + \bar{q}(x)] \quad (1)$$

$$g_1(x, Q^2) = \frac{1}{2} \sum_q e_q^2 [\Delta q(x) + \Delta \bar{q}(x)] , \quad (2)$$

where

$$q = q_\uparrow + q_\downarrow , \quad \Delta q = q_\uparrow - q_\downarrow . \quad (3)$$

The renewed interest in the subject was triggered by the first precision measurement of the integral of g_1^p by the EMC collaboration [2],

$$\Gamma_1^p(\text{EMC/SLAC}) \equiv \int_0^1 dx g_1^p(x, Q^2) = 0.126 \pm 0.010 \pm 0.015 \quad (Q^2 = 10 \text{ GeV}^2) , \quad (4)$$

which was significantly lower than the ‘Ellis-Jaffe sum rule’ value of 0.18 [3]. This latter prediction is obtained by assuming that the net contribution of strange quarks to the proton spin is negligible. In the context of this model, η_u and η_d , the net spin carried by up and down quarks respectively, can be obtained from the β -decay rates of the octet hyperons:

$$\begin{aligned} \eta_u &\equiv \int_0^1 dx \Delta u(x) = 2F \\ \eta_d &\equiv \int_0^1 dx \Delta d(x) = F - D . \end{aligned} \quad (5)$$

Attributing the difference between the Ellis-Jaffe prediction and the SLAC-EMC measurement to a non-zero strange sea polarization leads to the rather unusual result that the net spin carried by the quarks,

$$\eta_\Sigma \equiv \int_0^1 dx \Delta \Sigma(x) = \int_0^1 dx [\Delta u + \Delta d + \Delta s] , \quad (6)$$

is very small. This so-called ‘spin crisis’ precipitated an enormous amount of theoretical discussion – a clear and comprehensive review can be found in Ref. [4].

One of the most compelling explanations for the violation of the Ellis-Jaffe sum rule is that a substantial amount of the proton's spin is carried by *gluons*. As first pointed out in [5], the polarized gluon contributes to g_1 via the γ_5 -triangle anomaly. Thus in perturbative QCD, the naive parton model result of Eq. (2) is replaced by

$$\begin{aligned}
g_1(x, Q^2) &= \frac{1}{2} \sum_q e_q^2 \int_x^1 \frac{dy}{y} [\Delta q(x/y, Q^2) + \Delta \bar{q}(x/y, Q^2)] \\
&\times \left\{ \delta(1-y) + \frac{\alpha_s(Q^2)}{2\pi} \Delta C_q(y) + \dots \right\} \\
&+ \frac{1}{9} \int_x^1 \frac{dy}{y} \Delta G(x/y, Q^2) \left\{ n_f \frac{\alpha_s(Q^2)}{2\pi} \Delta C_G(y) + \dots \right\} \quad (7)
\end{aligned}$$

where $\Delta G = G_\uparrow - G_\downarrow$ is the polarized gluon distribution. Now according to the Altarelli-Parisi evolution equations [6],

$$\frac{d}{d \log Q^2} \eta_\Sigma(Q^2) = 0 + \mathcal{O}(\alpha_s^2) \quad (8)$$

$$\frac{d}{d \log Q^2} \alpha_s(Q^2) \eta_G(Q^2) = 0 + \mathcal{O}(\alpha_s^2), \quad (9)$$

which implies that the gluon contribution to g_1 is formally of the same order as the quark contribution. The splitting of the structure function into two conserved quantities associated with quark and gluon contributions to the net spin is natural in the sense that it allows the former to be identified (up to finite mass corrections) with the SU(6) ‘‘constituent’’ quarks. Retaining only the leading terms in Eq. (7), assuming three quark flavours, and using a factorization scheme where $\Delta C_G(y) = -\delta(1-y)$ (see Section 2), gives

$$g_1^p(x, Q^2) = \frac{1}{2} \sum_{q=u,d,s} e_q^2 [\Delta q(x, Q^2) + \Delta \bar{q}(x, Q^2)] - \frac{1}{3} \frac{\alpha_s(Q^2)}{2\pi} \Delta G(x, Q^2), \quad (10)$$

$$\Gamma_1^p = \int_0^1 dx g_1^p = \frac{2}{9} \eta_u + \frac{1}{18} \eta_d + \frac{1}{18} \eta_s - \frac{1}{3} \frac{\alpha_s(Q^2)}{2\pi} \eta_G. \quad (11)$$

It is now straightforward to calculate the amount of net gluon spin needed to explain the SLAC-EMC sum-rule data. For example, with $\eta_s = 0$ and η_u, η_d again obtained from hyperon decays, we find $\eta_G \sim 5$ at $Q^2 \sim 10 \text{ GeV}^2$ [7]. Although this might be considered a surprisingly large number there is no violation of spin conservation, since there is also a contribution to the proton's spin from the orbital angular momentum of the partons:

$$\frac{1}{2} = \frac{1}{2} \eta_\Sigma + \eta_G + \langle L_z \rangle. \quad (12)$$

According to Eq. (9), the second and third terms on the right-hand side increase as $\log Q^2$ in such a way that their sum is constant.

In Ref. [7] – hereafter referred to as AS – a simple leading-order QCD model, with no polarized strange sea at $Q^2 = Q_0^2 = 4 \text{ GeV}^2$, was used to extract polarized quark and gluon distributions from the SLAC and EMC data on $g_1^p(x, Q^2)$. Although the integrated parton distributions were reasonably well determined, the shapes of the distributions, especially those of the d -quark and the gluon, were poorly constrained. As a result, counting-rule and Regge arguments for the large and small x behaviour had to be invoked. The main purposes of the exercise were (i) to show that a consistent set of distributions could be derived, and (ii) to present parton distributions which could be used for polarized lepton-hadron and hadron-hadron collision phenomenology.

Since the AS analysis was performed, there has been a dramatic increase in the amount of polarized structure function data available. Using a polarized ^3He target, the E142 collaboration at SLAC has measured the neutron structure function g_1^n [8]. The SMC collaboration at CERN first measured the deuteron structure function g_1^d [9] and more recently has measured g_1^p [10], improving on the earlier SLAC-EMC measurements. These new results allow a test of another important sum rule due to Bjorken [11]

$$\Gamma_{\text{Bj}} \equiv \int_0^1 dx (g_1^p(x, Q^2) - g_1^n(x, Q^2)) = \frac{g_A}{g_V} \left[1 - \frac{\alpha_s(Q^2)}{\pi} + \dots \right]. \quad (13)$$

This sum rule follows from SU(2) isospin invariance and is a rigorous prediction of QCD. Any disagreement between the measured and predicted values would invalidate the QCD-improved parton model approach on which the present study is based. The most recent experimental measurement – using all available data [10] – gives

$$\Gamma_{\text{Bj}}^{\text{exp}} = 0.163 \pm 0.017 \quad (Q^2 = 5 \text{ GeV}^2), \quad (14)$$

to be compared to the third-order QCD prediction [12]

$$\Gamma_{\text{Bj}}^{\text{th}} = 0.185 \pm 0.004 \quad (Q^2 = 5 \text{ GeV}^2). \quad (15)$$

The agreement is acceptable, especially considering that higher-twist contributions might still give a small contribution at this Q^2 . In our parton distribution analysis, therefore, we shall use isospin symmetry to relate the distributions in the proton to those in the neutron.

It is interesting that the new measurement of the integrated proton structure function [10], again using all available data,

$$\Gamma_1^p(\text{SMC/EMC/SLAC}) = 0.142 \pm 0.008 \pm 0.011 \quad (Q^2 = 10 \text{ GeV}^2), \quad (16)$$

is larger than the old SLAC-EMC result. This means that our polarized gluon distribution (which accounts for the difference between the measured value and the Ellis-Jaffe prediction) will now be somewhat smaller than previous estimates: in fact we shall show below that¹ $\eta_G \sim 2$, compared to the AS result $\eta_G \sim 5$.

The goal of the present study is to use the latest available data to update and improve the AS parton distribution analysis. Following AS, we adopt the point of view that there should be no significant polarization of the strange quark sea. Although the sum-rule measurements give an indication of the size of η_G , there is a large arbitrariness in the *shape* of the gluon distribution. We will explore several qualitatively different shapes allowed by the data. The outcome of the analysis will again be a set of distributions which will provide benchmarks for future deep inelastic scattering experiments and which will be useful for phenomenological analyses of other types of polarized scattering experiment.

As we have already indicated, the first moments of our parton distributions are constrained by hyperon decay and sum-rule data. In the remainder of this section, we describe the input data which we use, and the corresponding first moments which obtain.

The structure function g_1^p occurs in the antisymmetric part of the hadronic tensor in deep inelastic scattering, which can be expressed as the matrix element of the axial vector current between two proton states [11]. These matrix elements can be further decomposed into the $SU(3)_f$ singlet and octet pieces. In order to compare the sum rules with experiment and to perform a Q^2 evolution of the polarized parton densities, we rewrite Eq. (10) as

$$g_1^p = \frac{1}{12}\Delta q_3(x, Q^2) + \frac{1}{36}\Delta q_8(x, Q^2) + \frac{1}{9}\Delta\Sigma(x, Q^2) - \frac{1}{3}\frac{\alpha_s(Q^2)}{2\pi}\Delta G(x, Q^2) \quad (17)$$

with similar expressions for the neutron and deuteron:

$$g_1^n = -\frac{1}{12}\Delta q_3(x, Q^2) + \frac{1}{36}\Delta q_8(x, Q^2) + \frac{1}{9}\Delta\Sigma(x, Q^2) - \frac{1}{3}\frac{\alpha_s(Q^2)}{2\pi}\Delta G(x, Q^2) \quad (18)$$

$$g_1^d = \frac{1}{36}\Delta q_8(x, Q^2) + \frac{1}{9}\Delta\Sigma(x, Q^2) - \frac{1}{3}\frac{\alpha_s(Q^2)}{2\pi}\Delta G(x, Q^2) . \quad (19)$$

Here we have defined octet and singlet quark distributions:

$$\begin{aligned} \Delta q_3 &= \Delta u - \Delta d \\ \Delta q_8 &= \Delta u + \Delta d - 2\Delta s \\ \Delta\Sigma &= \Delta u + \Delta d + \Delta s . \end{aligned} \quad (20)$$

The first moments of (17)-(19) are:

$$\Gamma_1^p = I_3 + I_8 + I_0 - \frac{1}{3}\frac{\alpha_s(Q^2)}{2\pi}\eta_G$$

¹using also improved F and D values

$$\begin{aligned}
\Gamma_1^n &= -I_3 + I_8 + I_0 - \frac{1}{3} \frac{\alpha_s(Q^2)}{2\pi} \eta_G \\
\Gamma_1^d &= I_8 + I_0 - \frac{1}{3} \frac{\alpha_s(Q^2)}{2\pi} \eta_G.
\end{aligned} \tag{21}$$

The axial-vector current matrix elements, I_3 and I_8 , are related to the F and D couplings:

$$\begin{aligned}
I_3 &= \frac{1}{12}(F + D) \\
I_8 &= \frac{1}{36}(3F - D).
\end{aligned} \tag{22}$$

Assuming $\eta_s = 0$ gives $I_0 = 4I_8$, leading to separate predictions for the quark contributions to the Γ_1 's [3].

Measuring F and D in hyperon β -decays gives their values at a momentum transfer scale of $Q^2 \approx \mathcal{O}(0.5 \text{ GeV}^2)$. However F and D , being related to the octet axial vector current matrix elements, are Q^2 dependent. To fix η_u and η_d for our fits, we incorporate these perturbative corrections by replacing F and D by \tilde{F} and \tilde{D} , which are obtained by comparing the parton model expressions for I_3 and $I_8 + I_0$ with their values corrected to first order in perturbative QCD. Demanding that \tilde{F} and \tilde{D} reproduce the corrected values of I_3 and $I_8 + I_0$, one has, following [13],

$$\begin{aligned}
\tilde{I}_3 = \frac{1}{12}(\tilde{F} + \tilde{D}) &= \frac{1}{12}(F + D) \left[1 - \frac{\alpha_s}{\pi} \right] \\
\tilde{I}_8 + \tilde{I}_0 = \frac{5}{36}(3\tilde{F} - \tilde{D}) &= \frac{1}{36}(3F - D) \left[\left(1 - \frac{\alpha_s}{\pi}\right) + 4\left(1 - \frac{\alpha_s}{3\pi}\right) \right].
\end{aligned} \tag{23}$$

This leads to

$$\begin{aligned}
\tilde{F} &= \left(1 - \frac{3\alpha_s}{5\pi}\right)F - \frac{2\alpha_s}{15\pi}D \\
\tilde{D} &= \left(1 - \frac{13\alpha_s}{15\pi}\right)D - \frac{2\alpha_s}{5\pi}F.
\end{aligned} \tag{24}$$

Taking $n_f = 3$ and $\Lambda = 177 \text{ MeV}$ (see below), we calculate \tilde{F} and \tilde{D} at the starting point of our perturbative evolution $Q_0^2 = 4 \text{ GeV}^2$ ($\alpha_s(4 \text{ GeV}^2) = 0.2879$), taking the experimental values for F and D from Ref. [13]:

$$\begin{aligned}
\tilde{F} &= 0.424 \pm 0.008 \\
\tilde{D} &= 0.718 \pm 0.007,
\end{aligned} \tag{25}$$

which fixes the first moments of the polarized u - and d -quark distributions:

$$\begin{aligned}
\eta_u &= 0.848 \pm 0.016 \\
\eta_d &= -0.294 \pm 0.011.
\end{aligned} \tag{26}$$

Finally, comparing the parton model expression for Γ_1^p (11) with the experimental value (16) gives

$$\eta_G = 1.971 \pm 0.929 . \quad (27)$$

The above result for the moments and the sum rules are summarized in Table (1).

partons	η_u	0.848 ± 0.016
	η_d	-0.294 ± 0.011
	η_s	0.000
	η_Σ	0.554 ± 0.019
	η_G	1.971 ± 0.929
g_1 (4 GeV ²)	Γ_1^p	0.142 ± 0.015
	Γ_1^n	-0.048 ± 0.015
	Γ_1^d	0.047 ± 0.015
	$\Gamma_1^p - \Gamma_1^n$	0.190 ± 0.002

Table 1: First moments of the quark and gluon parton distributions and of g_1

The remainder of the paper is organized as follows. In the next section we discuss the different possible definitions of the polarized gluon distribution. In Section 3 we describe our fit to the polarized structure function data, in Section 4 we discuss the implications of our fits for the polarized sea quark distributions at higher Q^2 , and in Section 5 we summarize our results and present our conclusions.

2 Definition of the polarized gluon distribution

The form of $\Delta C_G(x)$ in Eq. (7) has been a matter of some dispute during the past few years [4, 14, 15]. Kodaira [16] first pointed out that the anomalous dimension of the singlet axial vector current was non-zero. According to Ref. [16], the first moment of $\Delta C_G(x)$ is

$$\int_0^1 dx \Delta C_G(x) = -1. \quad (28)$$

Based on these ideas, Altarelli and Ross [5] evaluated the anomalous gluonic contribution to g_1 . A crucial point in this calculation is the regularization of collinear singularities (from

$g \rightarrow q\bar{q}$) in the photon-gluon fusion process. Depending on the regularization procedure used, one obtains different expressions for $\Delta C_G(x)$. In Ref. [5] the physical quark mass was used as a regulator, giving

$$\Delta C_G(x) = (2x - 1) \ln \frac{1-x}{x}. \quad (29)$$

The scheme dependence of $\Delta C_G(x)$ was further discussed by Bodwin and Qiu [14]. They obtained the surprising result that, in dimensional regularization and for finite quark masses, the first moment of $\Delta C_G(x)$ vanishes. Only the (unphysical) approach of assuming a small but finite gluon mass reproduced the result of [16]. A careful reanalysis [15] of the polarized photon-gluon fusion process showed that in fact this disagreement between different regularization schemes comes from the soft non-perturbative region. Contributions from this region should be absorbed into the light quark density, and should therefore not contribute explicitly to $\Delta C_G(x)$. This leaves us with two different possible $\Delta C_G(x)$, both with first moment equal to -1 . The first is obtained by introducing a non-zero gluon mass, while the second derives from either introducing finite quark masses or from applying dimensional regularization, always subtracting the soft contribution:

$$\Delta C_G(x) (k^2 < 0) = (2x - 1) \left(\ln \frac{1}{x^2} - 2 \right), \quad (30)$$

$$\Delta C_G(x) (\text{DR}, m^2 \neq 0) = (2x - 1) \left(\ln \frac{1-x}{x} - 1 \right). \quad (31)$$

The gluon contribution to g_1 , Eq. (7), involves the convolution of $\Delta C_G(x)$ with ΔG . Rather than tying ourselves to a particular theoretical scheme, we adopt the AS procedure [7] and define a “ g_1 -scheme” gluon with $\Delta C_G(x) = -\delta(1-x)$. Since only the first moments of the polarized quark and gluon densities are precisely defined, we are free to fix the higher moments in this way to obtain the simplest form for the gluon term in Eq. (7). Of course, in a consistent next-to-leading order analysis, any change in the definition of ΔC_G is compensated by a corresponding change in the $\mathcal{O}(\alpha_s)$ correction to the quark contribution, Eq. (7), in such a way that the physical quantity g_1 is scheme independent. A different choice of ΔC_G will then yield a different gluon *and* a different set of quark distributions. We are aware of the fact that our mixture of leading-order quark and next-to-leading order gluon contributions in g_1 is ambiguous. Nevertheless we consider the incorporation of the anomalous gluon, although formally of order α_s , to be motivated by the scaling behaviour of $\alpha_s \Delta G$ and by the magnitude of this contribution to g_1 . When complete next-to-leading order corrections become available it will of course be necessary to perform calculations of different processes within a consistent scheme.

Within our leading-order approach, it is straightforward to relate gluon distributions defined according to different schemes. Suppose that one uses a different coefficient func-

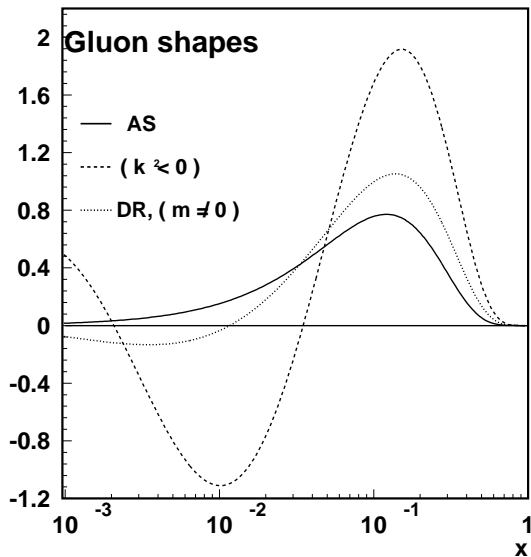


Figure 1: ΔG in different regularization schemes reproducing our (AS) set A gluon at Q_0^2 .

tion, $\Delta\tilde{C}_G(x)$ say, in the definition of g_1 . Then the corresponding polarized gluon distribution $\Delta\tilde{G}(x)$ (i.e. the distribution which reproduces the same g_1 at Q_0^2) is related to ours by

$$\Delta G(x, Q_0^2) = - \int_x^1 \frac{dy}{y} \Delta\tilde{G}\left(\frac{x}{y}, Q_0^2\right) \Delta\tilde{C}_G(y). \quad (32)$$

This equation can be inverted in Mellin moment space. Applying a Mellin transformation to Eq. (32) and defining

$$\Delta G(n) = \int_0^1 dx x^{n-1} \Delta G(x, Q_0^2) \quad (33)$$

$$\Delta\tilde{C}_G(n) = \int_0^1 dx x^{n-1} \Delta\tilde{C}_G(x), \quad (34)$$

we obtain

$$\Delta\tilde{G}(x, Q_0^2) = \frac{1}{2\pi i} \int_{a-i\infty}^{a+i\infty} dn x^{-n} \frac{\Delta G(n)}{\Delta\tilde{C}_G(n)}. \quad (35)$$

For reference, we list in Table 2 the Mellin moments of the coefficient functions of Eqs. (30) and (31).

In the following section, we will determine a polarized gluon distribution at Q_0^2 from a fit to the structure function data. The gluon defined in any other scheme can then be

obtained by numerical integration of Eq. (35). As an example, Figure 1 shows our gluon set A (see below) together with the two distributions which correspond to the different coefficient functions defined in Eqs. (30) and (31).

$\Delta C_G(x)$	$\Delta C_G^{(1)}$	Mellin transformation $\Delta C_G(n)$
$-\delta(1-x)$ (AS assumption)	-1	-1
$(2x-1)(\ln \frac{1}{x^2} - 2)$ ($k^2 < 0$)	-1	$-2 \frac{n^3 - n^2 + n + 1}{n^2(n+1)^2}$
$(2x-1)(\ln \frac{1-x}{x} - 1)$ (DR, $m^2 \neq 0$)	-1	$-\frac{n^3 + n^2 + n + 1 + (n^3 - n)(\gamma_E + \Psi(n+1))}{n^2(n+1)^2}$

Table 2: The different gluon coefficient functions and their Mellin transformations

3 Fit to the polarized structure function data

3.1 Parametric form of the fit

As a result of over twenty years of experiments, the *unpolarized* parton distributions in the proton are very precisely known, see for example Ref. [17]. Some twenty independent parameters are needed to specify the various quark and gluon distributions at Q_0^2 . In comparison, measurements of the polarized distributions are still rather imprecise. It is therefore necessary to build in to the parametrizations a significant amount of theoretical prejudice. As measurements improve in the future, these expectations will be tested and refinements can be made.

At present, the only constraints on the distributions are (i) the specification of the first moments of the distributions, as described in the Introduction and summarized in Table 1, and (ii) the requirements of *positivity* of the individual spin-parallel and spin-antiparallel distributions:

$$f_{\uparrow\downarrow} = \frac{1}{2}(f \pm \Delta f) > 0 \quad \Rightarrow \quad |\Delta f| \leq f, \quad (f = q, G). \quad (36)$$

Therefore, the absolute value of a polarized parton distribution always has to be smaller than the corresponding unpolarized distribution. We therefore require a consistent set

of leading-order unpolarized distributions to provide the bounds – those of Ref. [18] are ideal for this purpose. The starting distributions are, at $Q^2 = Q_0^2 = 4 \text{ GeV}^2$,

$$\begin{aligned}
x(u_v + d_v) &= N_{ud}x^{0.6650}(1-x)^{3.6140}(1+0.8673x) \\
xd_v &= N_d x^{0.8388}(1-x)^{4.6670} \\
x\bar{u} = x\bar{d} = x\bar{s} &= 0.1515(1-x)^{7.278} \\
xc &= 0 \\
xG &= 3.0170(1-x)^{5.3040}
\end{aligned} \tag{37}$$

and the evolution is performed with $\Lambda \equiv \Lambda_{\text{LO}}^{(4)} = 177 \text{ MeV}$. The parameters N_{ud} and N_d are fixed by the requirement that $\int_0^1 dx u_v = 2 \int_0^1 dx d_v = 2$.

For consistency, we choose the same Λ and Q_0 values as [18], and similar starting parametrizations. Only our choice of performing the whole evolution with three quark flavours differs from [18]. As explained in the Introduction, we start at Q_0 with valence-like forms for the up and down quarks and with an unpolarized sea:

$$\begin{aligned}
x\Delta u_v &= \eta_u A_u x^{a_u}(1-x)^{b_u}(1+\gamma_u x) \\
x\Delta d_v &= \eta_d A_d x^{a_d}(1-x)^{b_d}(1+\gamma_d x) \\
x\Delta\bar{u} = x\Delta\bar{d} = x\Delta\bar{s} &= 0 \\
x\Delta c &= 0 \\
x\Delta G &= \eta_G A_G x^{a_G}(1-x)^{b_G}(1+\gamma_G x)
\end{aligned} \tag{38}$$

with normalization factors A_f ($f = q, G$) to ensure that $\int_0^1 dx \Delta f(x, Q_0^2) = \eta_f$:

$$A_f^{-1} = \left(1 + \gamma_f \frac{a_f}{a_f + b_f + 1}\right) \frac{\Gamma(a_f)\Gamma(b_f + 1)}{\Gamma(a_f + b_f + 1)}. \tag{39}$$

Non-zero polarized SU(3) symmetric sea quark distributions are generated dynamically for $Q > Q_0$ (see below). Note that (i) the positivity constraints (36) demand that the b_f parameter values are at least as big as the corresponding unpolarized parameters of Eq. (37), and (ii) the convergence of the first moment integrals requires $a_f > 0$.

Even with these constraints, there are still too many free parameters in (38) for the amount of data available. We therefore impose additional theoretical constraints at large and small x , based on dimensional counting and coherence/Regge arguments respectively [19, 20, 21, 22, 23]. A good discussion of these can be found in Ref. [23]. In the present context, they can be summarized as follows:

- (i) The assumption that the small x behaviour of the quark distributions is controlled by Regge behaviour requires $a_u = a_d$.

- (ii) Coherence arguments at small x give $a_G^{pol} = a_G^{unpol} + 1$ for the gluon distribution.
- (iii) Spectator quark counting rules for the $x \rightarrow 1$ behaviour suggest $b_d = b_u + 1$ and require b_u and b_d to be the same as in the unpolarized case.

We have already mentioned that the most accurate data at present are for g_1^p . This means that the detailed shape of the d -quark and gluon distribution cannot yet be determined. Thus for the former we impose $\gamma_u = \gamma_d$, and for the latter we suggest three qualitatively different forms, defined by

$$\begin{aligned}
\text{Gluon A: } \quad \gamma_G &= 0.0 \\
\text{Gluon B: } \quad \gamma_G &= 18.0 \\
\text{Gluon C: } \quad \gamma_G &= -3.5
\end{aligned} \tag{40}$$

The reasoning behind these choices is as follows: $\gamma_G = 0$ (the ‘standard’ form) will give a fit with $G_\uparrow \sim G_\downarrow$ at large x , which corresponds to a fast-moving gluon being equally likely to have its spin parallel or antiparallel to the parent proton; γ_G large and positive will lead to $G_\uparrow \gg G_\downarrow$ at large x , i.e. a fast-moving gluon which is preferentially polarized in the direction of the proton’s spin; γ_G large and negative will give a large- x gluon whose spin is anticorrelated with that of the proton. For the latter two cases, we limit the absolute size of the parameter γ_G to ensure positivity of both G_\uparrow and G_\downarrow , and in each case we fit for the remaining parameter b_g .

Table 3 lists the parameters which are fixed by the above theoretical considerations. In Section 3.3 we describe how the remaining parameters a_u , γ_u and b_G are determined from the data.

Parameter	Value	Comments
b_u	3.64	unpolarized b_u [18]
b_d	4.64	unpolarized b_d [18]
a_G	1.000	coherence arguments[21]
η_u	0.848	$\eta_u = 2\tilde{F}$
η_d	-0.294	$\eta_d = \tilde{F} - \tilde{D}$
η_G	1.971	from Γ_1^p

Table 3: Parameters fixed by theory

3.2 Evolution of the parton distributions

Having fixed the starting distributions at $Q_0^2 = 4 \text{ GeV}^2$, the distributions at higher Q^2 are obtained from the leading-order evolution equations [6]:

$$\begin{aligned}
\frac{d\Delta\Sigma(x, Q^2)}{d \ln Q^2} &= \frac{\alpha(Q^2)}{2\pi} \int_x^1 \frac{dy}{y} \left[\Delta\Sigma(y, Q^2) \Delta P_{qq} \left(\frac{x}{y} \right) + \Delta G(y, Q^2) \Delta P_{qG} \left(\frac{x}{y} \right) \right] \\
\frac{d\Delta G(x, Q^2)}{d \ln Q^2} &= \frac{\alpha(Q^2)}{2\pi} \int_x^1 \frac{dy}{y} \left[\Delta\Sigma(y, Q^2) \Delta P_{Gq} \left(\frac{x}{y} \right) + \Delta G(y, Q^2) \Delta P_{GG} \left(\frac{x}{y} \right) \right] \\
\frac{d\Delta q_{val}(x, Q^2)}{d \ln Q^2} &= \frac{\alpha(Q^2)}{2\pi} \int_x^1 \frac{dy}{y} \left[\Delta q_{val}(y, Q^2) \Delta P_{qq} \left(\frac{x}{y} \right) \right]
\end{aligned} \tag{41}$$

where the splitting functions are

$$\begin{aligned}
\Delta P_{qq} &= \frac{4}{3} \left[\frac{1+z^2}{(1-z)_+} + \frac{3}{2} \delta(z-1) \right] \\
\Delta P_{qG} &= \frac{1}{2} [z^2 - (1-z)^2] \\
\Delta P_{Gq} &= \frac{4}{3} \frac{1 - (1-z)^2}{z} \\
\Delta P_{GG} &= 3 \left[(1+z^4) \left(\frac{1}{z} + \frac{1}{(1+z)_+} \right) - \frac{(1-z)^3}{z} + \left(\frac{11}{6} - \frac{n_f}{9} \right) \delta(1-z) \right].
\end{aligned} \tag{42}$$

With the first moments ΔP_{qq}^1 and ΔP_{qG}^1 both being equal zero it follows that

$$\eta_q = \int_0^1 dx \Delta q_{val}(x, Q^2) \quad \text{and} \quad \eta_\Sigma = \int_0^1 dx \Delta\Sigma(x, Q^2) \tag{43}$$

are both independent of Q^2 . With $\Delta P_{Gq}^1 = 2$ and $\Delta P_{GG}^1 = \beta_0/2$, one finds, using the renormalization group equation,

$$\frac{d}{d \ln Q^2} \alpha_s(Q^2) \eta_G(Q^2) = O(\alpha_s^2) \quad \text{where} \quad \eta_G(Q^2) \equiv \int_0^1 dx \Delta G(x, Q^2), \tag{44}$$

and so Γ_1^p , Γ_1^n and Γ_1^d defined in Eq. (21) are independent of Q^2 in leading order.

3.3 Fitting procedure

In principle, five sets of g_1 structure function data are available for a global fit: the proton data from SLAC-Yale [1], EMC [2] and SMC [10], the neutron data from SLAC-E142 [8], and the deuteron data from SMC [9]. Our analysis, however, is based on a leading-twist

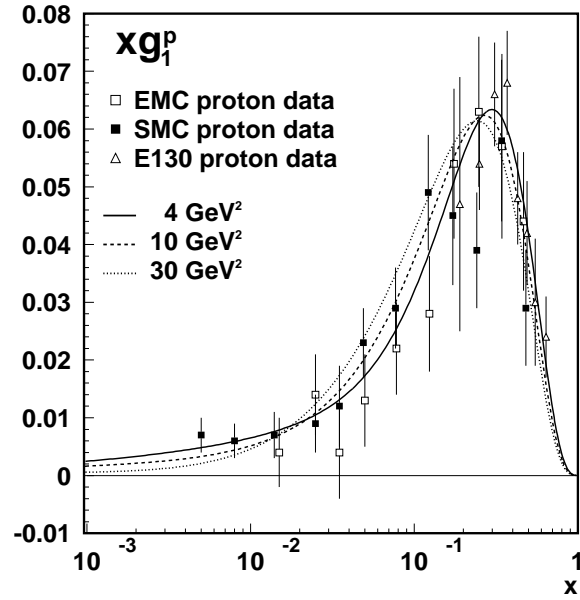


Figure 2: Fit to the g_1^p structure function with set A gluon

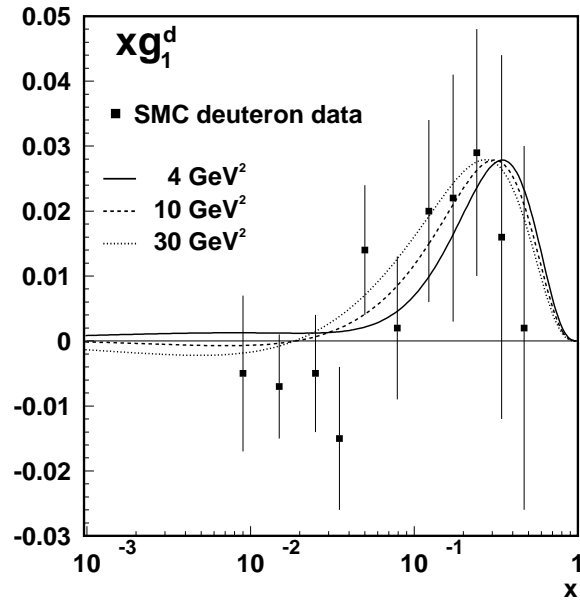


Figure 3: Prediction for the g_1^d structure function with the set A gluon

approximation, and it is therefore necessary to impose a minimum Q^2 cut. Based on similar fits to unpolarized structure function data, see for example [17], and on recent theoretical estimates [24, 25], we believe that $Q^2 \geq 4 \text{ GeV}^2$ is sufficient. This means that the bulk of the SLAC data ($E_{\text{beam}} = 30 \text{ GeV}$) falls outside our fit region. Only the EMC and SMC proton data ($E_{\text{beam}} \approx 200 \text{ GeV}$) cover a broad range of x for $Q^2 \geq 4 \text{ GeV}^2$.

The results of the fit are shown in Figs. 2 and 3. It turns out that the errorbars on the deuteron data are so large that there is no statistically significant constraint. The fit to g_1^p , Fig. 2, is equally good for the three different types of gluon distribution described in Section 3.1 (see Table 4), and so only the curves corresponding to set A are shown. Each data point is fitted at its appropriate x and Q^2 value, but since data from different beam energies are shown on the same figure, the curves correspond to fixed $Q^2 = 4, 10, 30 \text{ GeV}^2$. For the SMC and EMC data, these correspond to the small-, medium- and large- x data respectively. For the SLAC data, only the largest x data points have $Q^2 \sim 4 \text{ GeV}^2$. The lower x data points are not used in the fit but are displayed for completeness. Figure 4 shows our *predictions* for the neutron structure function, together with the SLAC-E142 data [8]. Only the largest x data point (with $Q^2 = 5.2 \text{ GeV}^2$) can be compared with the theoretical curves. At lower x , we might expect that higher-twist contributions are important, although it is interesting that the $Q^2 = 4 \text{ GeV}^2$ curve still gives a fair description of the data.

The values of the fitted parameters and their associated errors are listed in Table 4. Not surprisingly, the quark distributions are almost independent of the choice of gluon distribution and the quality of the fit is similar for sets A, B and C. Note that the a_u ($= a_d$) parameter is reasonably constrained to have a value $\simeq 0.45$, close to the corresponding unpolarized values, see (37).

	Gluon A	Gluon B	Gluon C
γ_G	0.0	18.0	-3.5
χ^2/dof	18.8/30	18.9/30	20.8/30
a_u	0.46 ± 0.15	0.45 ± 0.12	0.43 ± 0.12
γ_u	18.36 ± 14.49	20.22 ± 12.2	17.05 ± 10.71
b_G	7.44 ± 3.52	11.07 ± 4.19	8.00 ± 1.59

Table 4: The fitted parameters and χ^2/dof values corresponding to the three types of gluon distribution. Note that in each case $a_u = a_d$ and $\gamma_u = \gamma_d$.

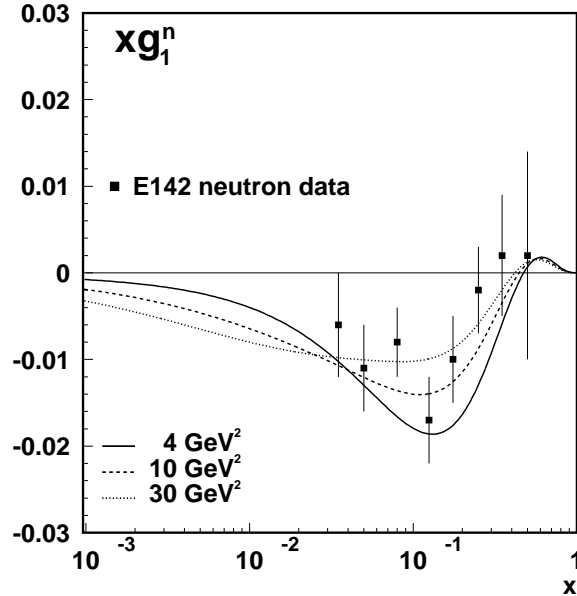


Figure 4: Prediction for the g_1^n structure function with the set A gluon

Figures 5-7 show the gluon, quark-singlet, u -valence and d -valence distributions at Q_0^2 obtained from the fits. For comparison, we show also the unpolarized distributions of Ref. [18].

A final comment concerns the shape of the gluon distribution at small x . For all of our sets, the gluonic contribution to g_1 is smooth and negative at small x . If one uses a different gluon coefficient function, for example either of those in Table 2, then the same smooth single-signed behaviour can only be reproduced by using an oscillating gluon, see Fig. 1. Conversely, a smooth gluon combined with either of these alternative coefficient functions would give a gluonic contribution to g_1 which changes sign at small x .

4 Predictions for $\Delta\bar{q}$

In our model, a non-zero antiquark distribution $\Delta\bar{q}$ is generated at higher Q^2 by the evolution of the quark singlet, Eq. (41). The resulting $\Delta\bar{q}$ is sensitive to the initial shape of the gluon. A measurement of the polarized sea-quark distribution for $Q^2 > 4 \text{ GeV}^2$ (recall that we generate an SU(3) symmetric sea) would therefore probe the gluon distribution. There are several ways that this could be done. Perhaps the most promising in the short term is to identify specific flavours of hadrons in the final-state. The extension of Eq. (2)

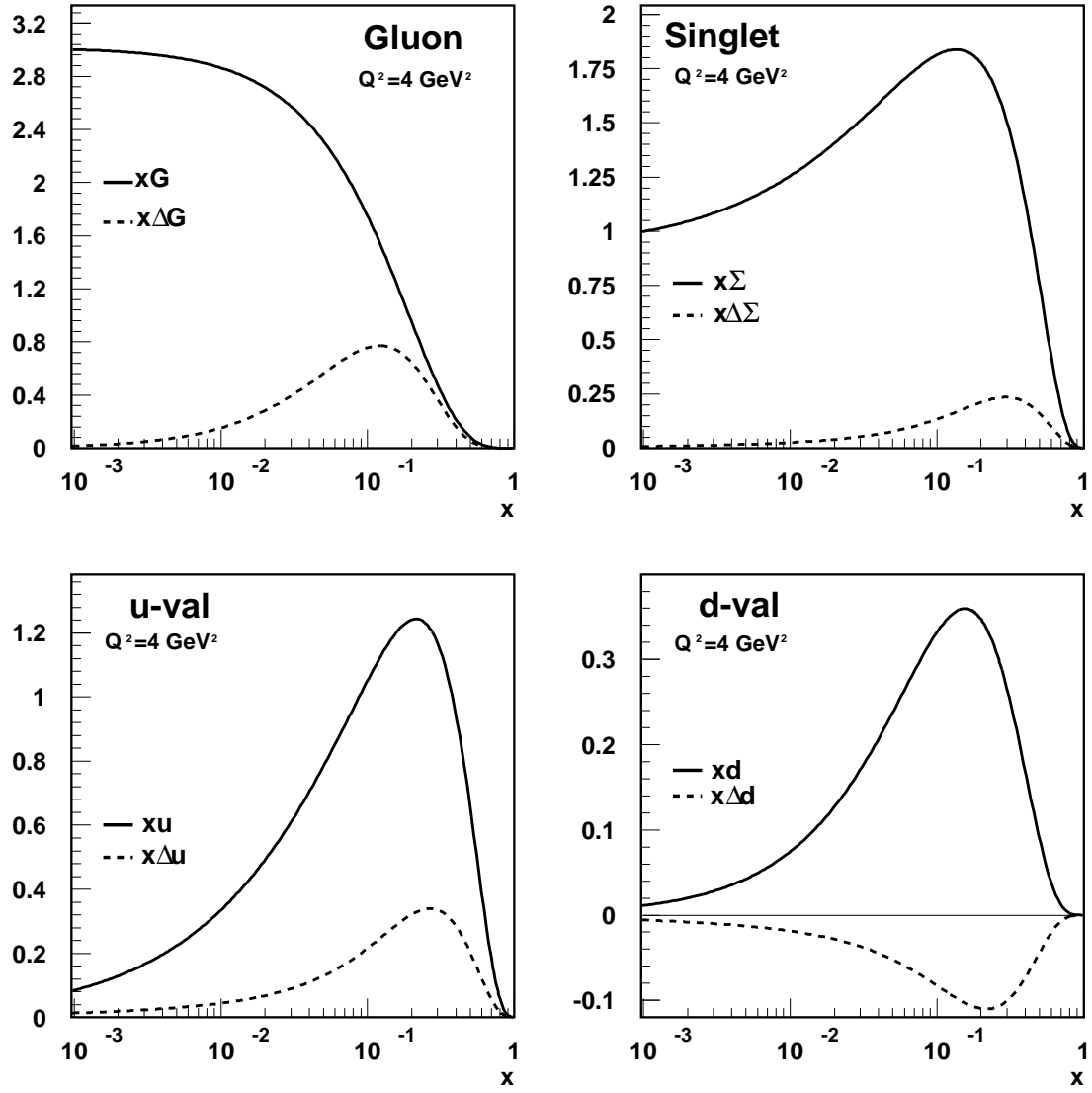


Figure 5: The polarized gluon (set A), quark singlet, u_v and d_v distributions at $Q_0^2 = 4 \text{ GeV}^2$ obtained from the fit to the deep inelastic scattering data.

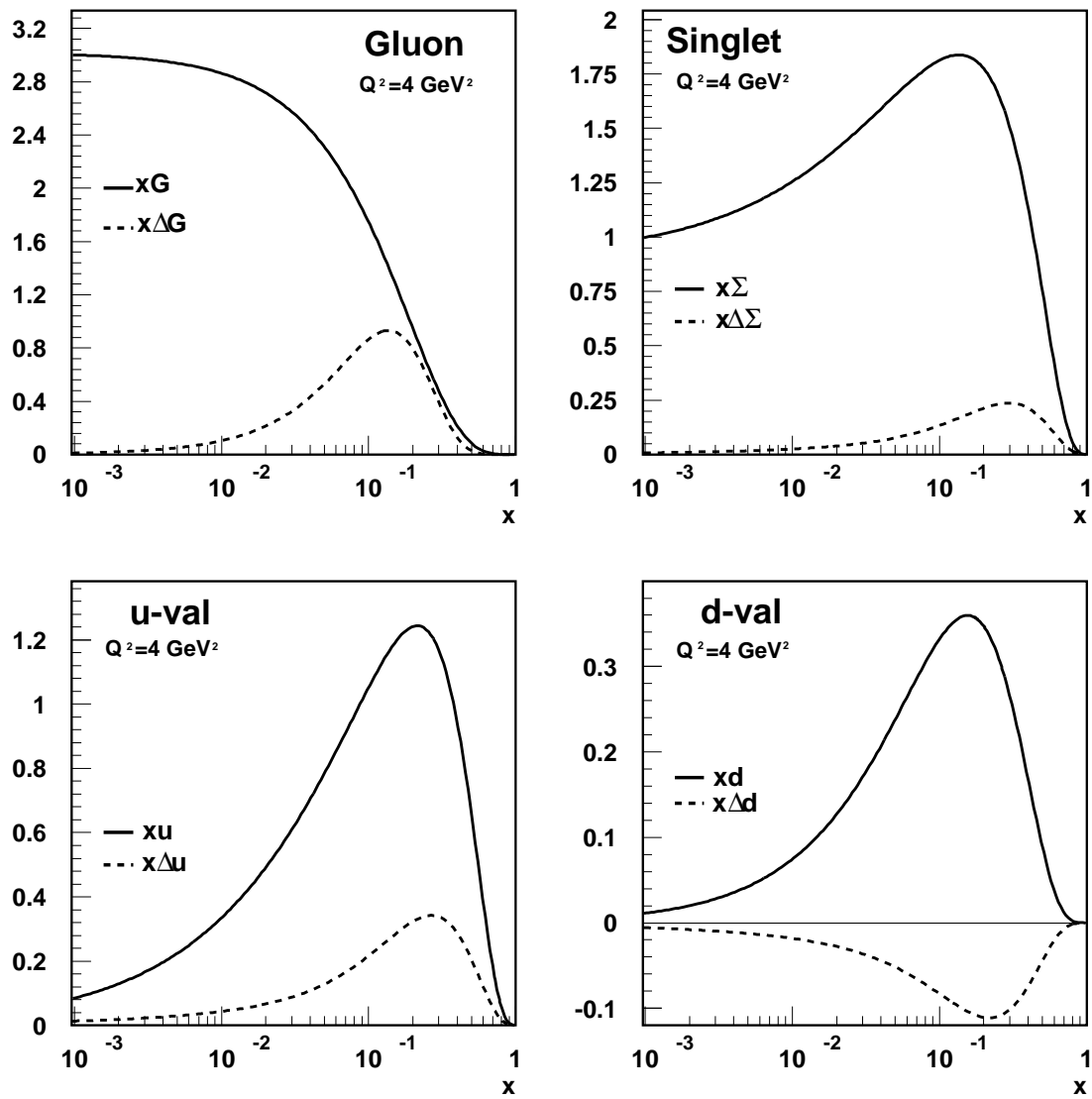


Figure 6: As for Fig. 5, but with the set B gluon distribution.

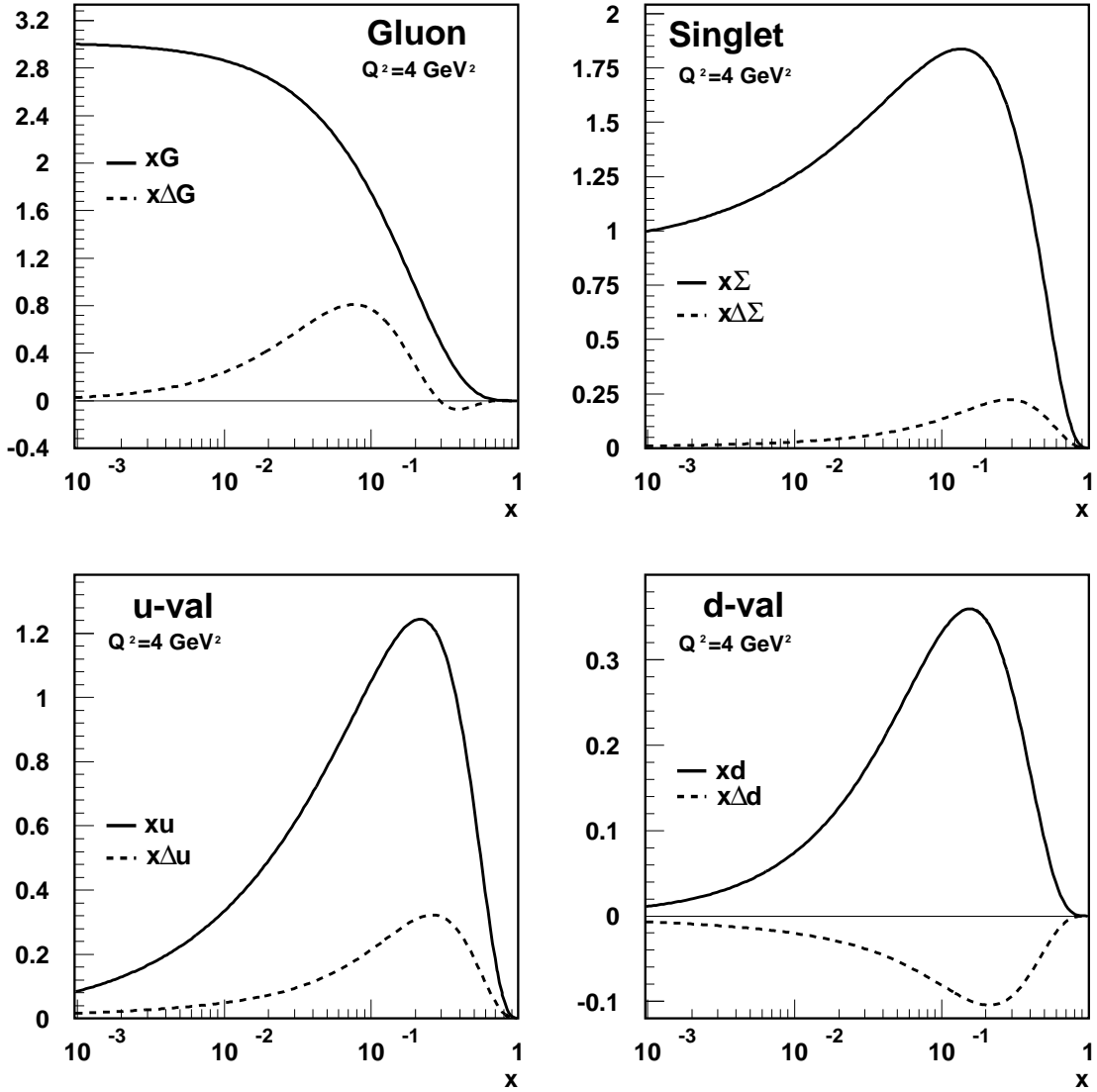


Figure 7: As for Fig. 5, but with the set C gluon distribution.

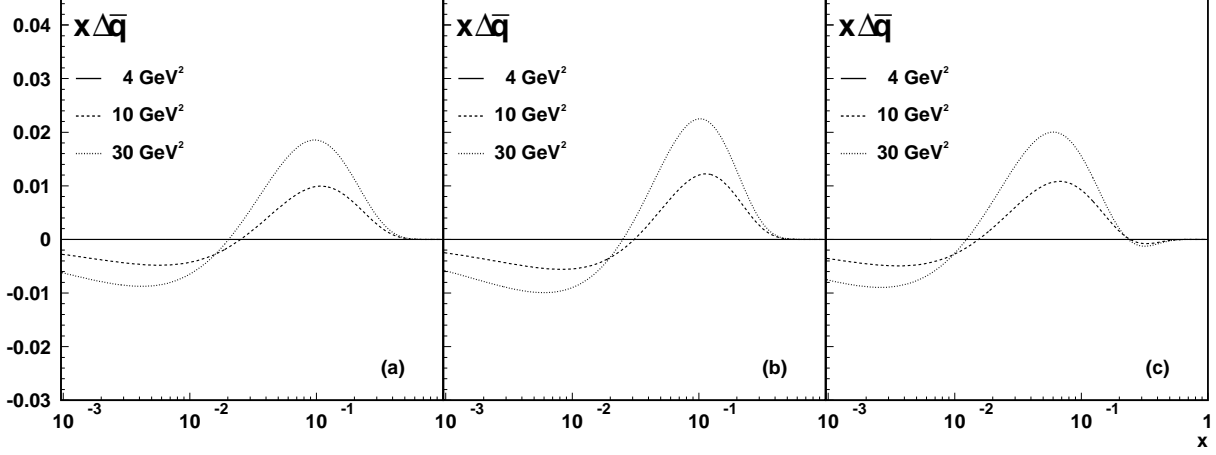


Figure 8: The $x\Delta\bar{q}$ distributions at $Q^2 = 4, 10, 30 \text{ GeV}^2$ corresponding to the (a) set A, (b) set B, and (c) set C gluon distributions.

to hadron inclusive structure functions for $lp \rightarrow lH + X$ is

$$F_1^{p \rightarrow H}(x, z, Q^2) = \frac{1}{2} \sum_q e_q^2 [q(x)D^{q \rightarrow H}(z) + \bar{q}(x)D^{\bar{q} \rightarrow H}(z)] \quad (45)$$

$$g_1^{p \rightarrow H}(x, z, Q^2) = \frac{1}{2} \sum_q e_q^2 [\Delta q(x)D^{q \rightarrow H}(z) + \Delta \bar{q}(x)D^{\bar{q} \rightarrow H}(z)], \quad (46)$$

where $D^{q \rightarrow H}(z)$ are fragmentation functions. As explained, for example, in Ref. [26], the identification of π^\pm, K^\pm, \dots in the final state allows the sea-quark polarization to be probed directly. Our predictions for the polarized sea-quark distribution are shown in Fig. 8. Independent of the choice of gluon, all the distributions have the common feature of being *negative* for small $x < \mathcal{O}(0.01)$. At large x , the fact that ΔG_C is less than zero (see Fig. 7) is reflected in the corresponding $\Delta\bar{q}_C$ distribution.

A preliminary study of the final-state hadron charge asymmetry in polarized deep inelastic scattering by SMC [27] has given a first indication of the size and shape of the $\Delta\bar{q}$ distribution. Although the experimental errors are still rather large, all the distributions of Fig. 8 are consistent with these data.

5 Summary and conclusions

In this paper we have described an attempt to perform a global fit to polarized deep inelastic structure function data on proton targets in order to extract a consistent set

of polarized parton distributions. We have adopted the point of view that there is no significant polarization of the sea quarks at low Q^2 , and therefore that the gluon carries a substantial fraction of the proton's spin. We have constrained the net spin carried by the various parton flavours using deep inelastic sum-rule and hyperon decay measurements. Recognizing that the quality of the data is not yet high enough to fully constrain the shapes of the distributions, we have imposed reasonable theoretical constraints at large and small x . We have performed fits with three qualitatively different gluon distributions, chosen to reflect the extent to which fast-moving gluons ‘remember’ the spin of the parent proton.

Our distributions have several applications:

- (i) they provide a benchmark for future deep inelastic structure function measurements – in particular, measurements using neutron and deuteron targets,
- (ii) they can be compared with theoretical, non-perturbative model calculations of the spin structure of the proton,
- (iii) they can be used to predict cross sections for the production of various flavours of hadrons in the final state – π^\pm and K^\pm for probing the quark sea, and the production of heavy quarks (in particular J/ψ and open charm) for probing the gluon distribution, and
- (iv) they can be used as input for the calculation of hard scattering cross sections in polarized hadron-hadron collisions.²

In conclusion, polarized lepton-hadron scattering experiments are beginning to provide precision information on how the spin of the proton is shared among its parton constituents. This will be invaluable in testing the predictions of Quantum Chromodynamics and in designing future experiments. Our distributions should be a useful tool in both these areas.³

Acknowledgements

We are grateful to R. Voss and W. Wislicki for useful discussions concerning the data. One of us (TG) would like to thank E. Reya for drawing his attention to this subject and for numerous clarifying and motivating discussions. This work was supported in part by Studienstiftung des deutschen Volkes, Bonn, and by the EEC Programme “Human Capital

²More details of these types of processes and references can be found in Ref. [4].

³A FORTRAN package containing the distributions can be obtained by electronic mail from T.K.Gehrmann@durham.ac.uk

and Mobility”, Network “Physics at High Energy Colliders”, contract CHRX-CT93-0537 (DG 12 COMA).

References

- [1] M.J. Alguard et al, SLAC-Yale collaboration: Phys. Rev. Lett. **37** (1976) 1261; G. Baum et al., SLAC-Yale collaboration: Phys. Rev. Lett. **45** (1980) 2000; **51** (1983) 1135.
- [2] J. Ashman et al., EMC collaboration: Nucl. Phys. **B328** (1989) 1.
- [3] J. Ellis and R.L. Jaffe: Phys. Rev. **D9** (1974) 1444, erratum **D10** (1974) 1669.
- [4] E. Reya, Proc. XXXII Internationale Universitätswochen für Kern- und Teilchenphysik, Schladming, Austria (1993), eds. L. Mathelitsch and W. Plessas, Springer-Verlag (1994) p.175.
- [5] G. Altarelli and G.G. Ross: Phys. Lett. **B212** (1988) 391.
- [6] G. Altarelli and G. Parisi: Nucl. Phys. **B126** (1977) 298.
- [7] G. Altarelli and W.J. Stirling: Particle World **1** (1989) 40.
- [8] D.L. Anthony et al., SLAC-E142 collaboration: Phys. Rev. Lett. **71** (1993) 959.
- [9] B. Adeva et al., SMC collaboration: Phys. Lett. **B302** (1993) 553.
- [10] D. Adams et al., SMC collaboration: Phys. Lett. **B329** (1994) 399.
- [11] J.D. Bjorken: Phys. Rev. **148** (1966) 1467, Phys. Rev. **D1**. (1970) 1376
- [12] S.A. Larin and J.A.M. Vermaseren: Phys. Lett. **B259** (1991) 345.
- [13] F.E. Close and R.G. Roberts: Phys. Lett. **B316** (1993) 165.
- [14] G.T. Bodwin and J. Qiu: Phys. Rev. **D41** (1990) 2755.
- [15] W. Vogelsang: Z. Phys. **C50** (1991) 275.
- [16] J. Kodaira: Nucl. Phys. **B165** (1979) 129.
- [17] A.D. Martin, R.G. Roberts and W.J. Stirling: Phys. Rev. **D47** (1993) 867.
- [18] J.F. Owens: Phys. Lett. **B266** (1991) 126.

- [19] J. Ellis and M. Karliner: Phys. Lett. **B213** (1988) 73, **B313** (1993) 131.
- [20] F.E. Close and R.G. Roberts: Phys. Rev. Lett. **60** (1988) 1471.
- [21] S.J. Brodsky and I. Schmidt: Phys. Lett. **B234** (1990) 144.
- [22] P. Chiapetta and G. Nardulli: Z. Phys. **C51** (1991) 435.
- [23] S.J. Brodsky, M. Burkhardt and I. Schmidt: preprint SLAC-PUB-6087 (1994).
- [24] I.I. Balitsky, V.M. Braun and A.V. Kolesnichenko: Phys. Lett. **B242** (1990) 245, erratum **B318** (1993) 648.
- [25] X. Ji and P. Unrau: preprint MIT-CTP-2232 (1993).
- [26] F.E. Close and R.G. Milner: Phys. Rev. **D44** (1991) 3691.
- [27] SMC collaboration: W. Wislicki, Proc. XXIXth Rencontres de Moriond ‘QCD and High Energy Interactions’, Les Arcs 1994, in print.